Characteristics of an infrared sensor formed with a few molecular layers of vinylidene fluoride oligomers with in situ poling during vacuum evaporation

Sutani, Yohei ; Fukushima, Tatsuya ; Koshiba, Yasuko ; Horike, Shohei ; Kodani, Tetsuhiro ; Kanemura, Takashi ; Ishida, Kenji

(Citation)
Japanese Journal of Applied Physics,59(SD):SDDF01-SDDF01

(Issue Date)
2020-03-01

(Resource Type)
journal article

(Version)
Version of Record

Japanese Journal of Applied Physics

The Japan Society of Applied Physics

REGULAR PAPER • OPEN ACCESS

Characteristics of an infrared sensor formed with a few molecular layers of vinylidene fluoride oligomers with in situ poling during vacuum evaporation

OPEN ACCESS

Japanese Journal of Applied Physics **59**, SDDF01 (2020) **REGULAR PAPER**

https://doi.org/10.7567/1347-4065/ab5502

Characteristics of an infrared sensor formed with a few molecular layers of vinylidene fluoride oligomers with in situ poling during vacuum evaporation

Yohei Sutani[1], Tatsuya Fukushima[1], Yasuko Koshiba[1], Shohei Horike[1,2], Tetsuhiro Kodani[3], Takashi Kanemura[3], and Kenji Ishida[1*]

[1]*Department of Chemical Science and Engineering, Graduate School of Engineering, Kobe University, Kobe, Hyogo 657-8501, Japan*
[2]*National Institute of Advanced Industrial Science and Technology (AIST), 1-1-1 Higashi, Tsukuba, Ibaraki 305-8565, Japan*
[3]*DAIKIN Industries Ltd., Osaka 530-8323, Japan*

*E-mail: kishida@crystal.kobe-u.ac.jp

Received August 12, 2019; revised October 6, 2019; accepted November 6, 2019; published online December 12, 2019

Perpendicularly oriented vinylidene fluoride oligomer thin films with six molecular layers were poled during vacuum evaporation (in situ poling) using a micro-gapped comb-like electrode, and their pyroelectric characteristics were investigated. The extent of polarization achieved with in situ poling performed by applying a low electric field (7.7 MV m^{-1}) is the same as that achieved by conventional post-poling with the application of a high electric field (>100 MV m^{-1}). Despite using a film with a few molecular layers, the in situ poled sensor showed pyroelectric response without the use of an infrared ray absorption layer; voltage sensitivity of 198 V W^{-1} was obtained, which is much higher than that of the post-poled sensor (~16 V W^{-1}). The improvement in sensitivity is attributed to the amount of charge injected during the poling treatment.

1. Introduction

Many sensors around us are generally used to gather information that is referred to as "big data" on work efficiency, safety, security, environment, medicine, industry, agriculture, and social infrastructure.[1–4] In the near future, sensor-based big data are expected to bring new business opportunities, leading to better management of smart cities, healthcare services, environmental protection, and disaster monitoring. Among the different kinds of sensors, pyroelectric infrared sensors are non-contact-type thermal sensors that can detect human body, gas, and abnormal heat generation by receiving infrared rays emitted from humans and heat sources.[5–8] In general, pyroelectric sensors are composed of inorganic ferroelectric materials, such as lead zirconate titanate (PZT). Although PZT-based sensors exhibit good performance,[9,10] PZT contains Pb, the use of which is restricted by the Restriction of Hazardous Substances directive. It is therefore important to replace the toxic Pb-containing materials of sensors with eco-friendly ones toward the next-generation sensor world, in which a massive number of sensor devices are expected to be used.

Organic ferroelectric materials are one of the promising alternatives to PZT, because of their minimal environmental impact. Vinylidene fluoride (VDF) based organic ferroelectric materials exhibit relatively better ferroelectricity and pyroelectricity among organic ferroelectrics, because they have a large electric dipole moment generated from the difference in electronegativity between the fluorine and hydrogen atoms in the molecule. One of the most commonly used organic ferroelectrics that can be simply spin-coated to obtain thin films is the polymeric VDF material poly (vinylidene fluoride-trifluoroethylene) [P(VDF-TrFE)].[11] However, the remnant polarization (P_r) of P(VDF-TrFE) film is smaller than the theoretically predicted polarization (130 mC m^{-2}) based on the VDF crystal structure, because the structure of polymer aggregates in the film tends to become disordered, and crystalline and amorphous phases coexist, resulting in the limitation of P_r to a maximum of ~94 mC m^{-2}.[12] In comparison, VDF oligomers show the largest P_r of 130 mC m^{-2}.[13,14] Their pyroelectric coefficient (p) is higher at $-70\ \mu$C m^{-2} K than that of P(VDF-TrFE) ($p \sim -45\ \mu$C m^{-2} K), reflecting the superior P_r.[15,16]

Conventionally, a polarization treatment, which induces the alignment of dipoles in the film, is performed on pyroelectric sensors to achieve pyroelectricity. However, the polarization of VDF-based organic ferroelectrics after film formation (post-poling) requires a higher electric field of >100 MV m^{-1} than that used for the polarization of inorganic ferroelectrics (e.g. PZT ~4 MV m^{-1}).[17] This is because it is difficult for the reversal of polarization with the flipping of the VDF main chain to occur due to the spatial restriction around the main chain. Therefore, a VDF-based sensor has reliability issues such as dielectric breakdown when a high electric field is applied.[14]

Additionally, the VDF oligomer is a linear molecule with a molecular weight of ~2000 or lower; the main chain of the VDF oligomer can be easily aligned perpendicularly to the substrate above the room temperature, similar to that of an n-alkane.[18,19] In the case of conventional parallelly oriented VDF oligomer based sensors, an increase in the environmental temperature during the sensor operation sometimes leads to device breakdown and/or degradation of the sensor due to changes in the structure and morphology of the sensor film (a change in the molecular orientation from parallel to perpendicular).[20] Thus, in order to develop a pyroelectric sensor based on VDF oligomers with large p, it is necessary to fabricate highly crystalline thin films with perpendicularly oriented VDF oligomers, which have superior thermal stability. When the VDF oligomer is deposited above the room temperature, the main chain of the VDF oligomer is oriented perpendicularly to the substrate, and the polarization direction of the VDF oligomer is parallel to the substrate;[21] the requirement then is to fabricate the metal/pyroelectric

material/metal structure perpendicular to the substrate.[14] Therefore, a microelectrode structure capable of inducing an electric field in the in-plane direction is required, which we achieved by adopting a micro-gapped comb-like electrode structure.

In this study, we investigated the polarization process during vacuum evaporation, that is, "in situ poling", to improve the reliability of the sensor by restraining the production of defective sensors during the poling process. Yoshida et al. reported that P(VDF-TrFE) films evaporated under an electric field form ferroelectric Form I crystals, and the dipole moment is oriented normally to the substrate, from a structural viewpoint.[22] In addition, the structural ordering and ferroelectric performance of PVDF evaporated films under an electric field have been reported.[23,24] However, the structure and the dipole alignment of their ferroelectric polymer films are hard to control due to thermal decomposition, and so their ferroelectric and pyroelectric properties are not enough for use in practical applications. Here, structural and electrical characterization of in situ poled VDF oligomer thin films were conducted. As experimental results, we found that the dipoles of VDF oligomer molecules under nucleation and film growth could be aligned at a lower electric field (7.7 MV m^{-1}) than required for post-poling (>100 MV m^{-1}). Furthermore, the voltage sensitivity of a pyroelectric sensor formed with six layers of perpendicularly oriented VDF oligomers could be observed by the suppression of charge injection.

2. Experimental methods

A 5-nm-thick Cr film and 50-nm-thick Au film were deposited on a thermally oxidized Si wafer by vacuum evaporation. Laser lithography and subsequent wet etching were performed to pattern comb-like microelectrodes [Fig. 1(a)]. The distance between the electrodes was set to 1.3 μm [Fig. 1(b)]. Thin films of the VDF oligomer [$CF_3(CH_2CF_2)_{19}I$; Daikin Kogyo Co. Ltd.; Fig. 1(c)] were deposited on the comb-like microelectrodes by vacuum evaporation. The substrate temperature (T_s) was controlled at 373 K and "in situ poling" was conducted under a DC electric field of 7.7 MV m^{-1} (10 V) applied between the electrodes during the deposition of the VDF oligomer film by vacuum evaporation. After film formation, the film thickness was measured with a stylus profiler.

To examine the extent of polarization induced by "in situ poling", the current density–electric field (J–E) switching curves were acquired using a ferroelectric measurement system (TOYO Corporation FCE-1).

The molecular conformation and orientation were analyzed by Fourier transform infrared (FT-IR) spectroscopy (JASCO FT/IR-660 Plus) in reflection absorption spectrometry and transmission modes. The surface morphology was observed by tapping-mode atomic force microscopy (AFM; JEOL JSPM-5200).

To characterize the pyroelectricity of the film, a blackbody source was used to generate infrared radiation, which was modulated using a mechanical chopper with a frequency of 0.2–200 Hz. The pyroelectric current was amplified and converted into voltage using a voltage follower circuit, and the output voltage was monitored on an oscilloscope (Tektronix, Inc., TDS5034B). For the calculation of voltage sensitivity, frequency components were extracted from the output voltage using a lock-in amplifier (NF Corporation LI5640).

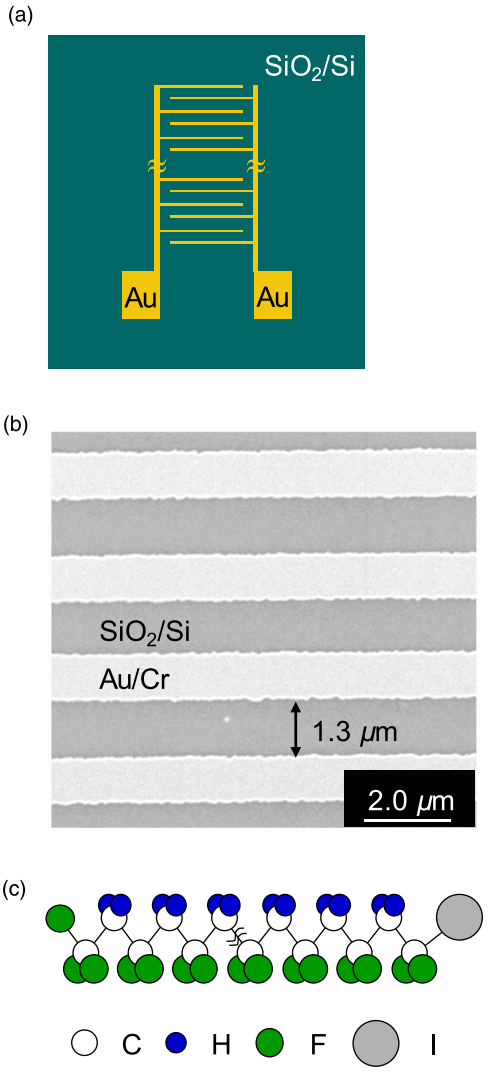

Fig. 1. (Color online) (a) Schematic and (b) SEM image of the comb-like electrodes fabricated on a SiO_2/Si substrate, and (c) schematic of the chemical structure of the VDF oligomer.

To examine the effects of different poling treatments, thermally stimulated current (TSC) was measured using a semiconductor parameter analyzer (Keysight Technologies B1500A). TSC was measured while increasing the temperature from 300 K to 353 K at a heating rate of 2 K min^{-1} under vacuum.

3. Results and discussion

Figures 2(a) and 2(b) show a cross-sectional drawing of our pyroelectric sensor structure and the film thickness profile, respectively. The film thickness of the VDF oligomer was about 30 nm. A film thickness of 30 nm corresponds to six molecular layers because the length of the VDF oligomer molecule used in this work was 4.8 nm.

To evaluate the extent of the polarization of VDF oligomer thin films under an applied electric field during their vacuum evaporation, we determined their ferroelectric properties, especially the extent of the polarization after in situ poling, which is presented in Fig. 3. A displacement current density of approximately ±50 A m^{-2} was observed in measurements

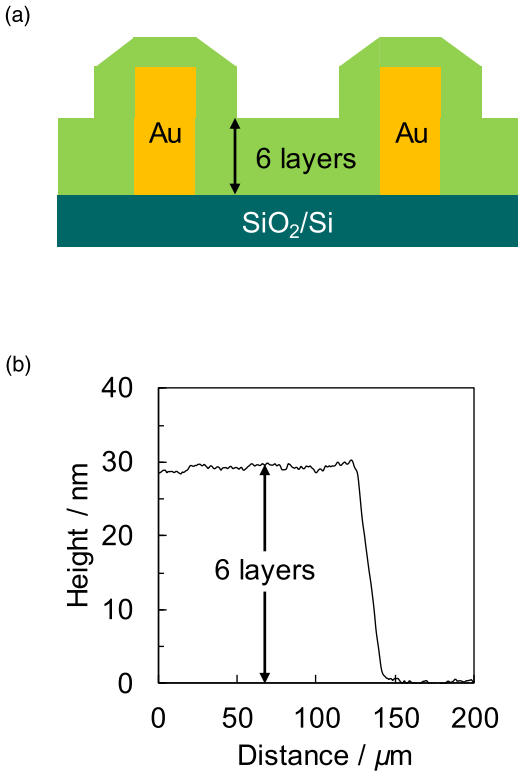

Fig. 2. (Color online) (a) A cross-sectional drawing of our pyroelectric sensor structure and (b) line profile of VDF oligomer thin films.

performed on a Au micro-gapped comb-like electrode on a Si substrate without the VDF oligomer film. For the device based on VDF oligomer film, the current density peak at $\sim$100 MV m^{-1} [position (II)] was caused by the reversal of the dipoles of molecules that did not align during film formation. The peak at approximately -80 MV m^{-1} [position (III)] is attributed to the reversal of almost all the dipoles. P_r was calculated from the difference in the areas of Peak II and Peak III (red hatch in the figure). The results indicate that the P_r of the in situ poled VDF oligomer thin film was 100 mC m^{-2}, which matches the P_r of a typical VDF oligomer film subjected to post-poling (>100 MV m^{-1}). However, in the case of the in situ poling, the electric field applied during film formation was 7.7 MV m^{-1}, which is much lower than the coercive electric field (E_c) of the VDF oligomer thin film at room temperature (E_c: 100–130 MV m^{-1}). Previous studies[14] have shown that E_c tends to decrease with increasing temperature, especially near the melting point of the thin film. Therefore, a high electric field was not required for the arrangement of the dipoles of the VDF oligomer, because of the high mobility of the oligomer in the gaseous state during vacuum evaporation and because the substrate temperature (T_s: 373 K) was close to the melting point of the oligomer (T_m: 443 K).

Figure 4 shows the FT-IR transmission and reflection absorption spectra of the VDF oligomer thin film obtained by deposition of the film under an electric field. The assignment of each infrared absorption band was made based on the FT-IR spectrum of PVDF having the same main-chain structure.[25–27] The distinct absorption peaks at 1413 cm^{-1} (CH_2 wagging) and 1073 cm^{-1} (C–C asymmetric stretching) indicate the formation of a ferroelectric I phase and the perpendicular orientation of the VDF oligomers with respect to the substrate, regardless of the presence or absence of an electric field. Therefore, the in situ poling process does not adversely affect the molecular orientation and crystal structure in the initial stage of film growth. Figure 5 shows the AFM images of the VDF oligomer films. Significant differences are not observed in the surface morphology of films deposited with and without an electric field during film formation. Plate-like grains are observed in the film formed

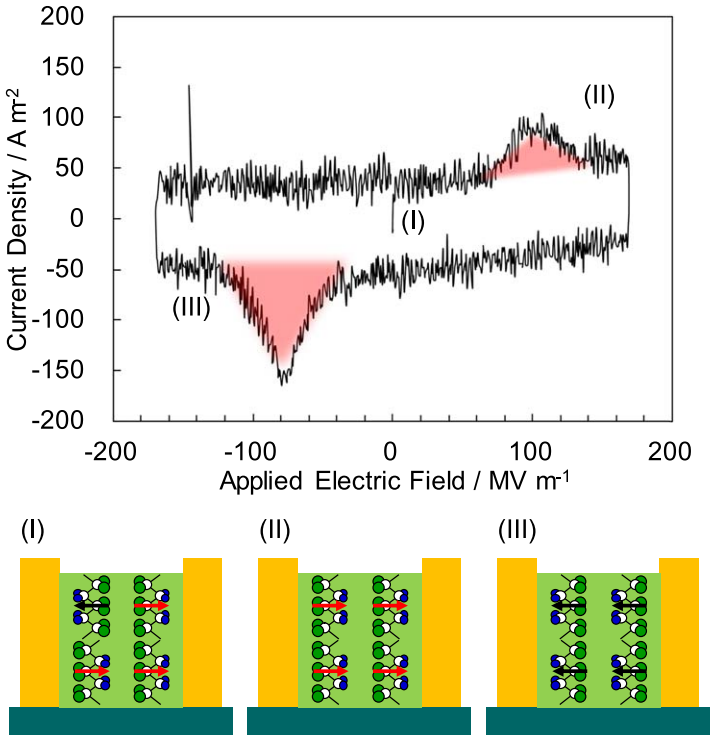

Fig. 3. (Color online) (a) *J*–*E* switching curve and (b) overview of in situ poled sensor.

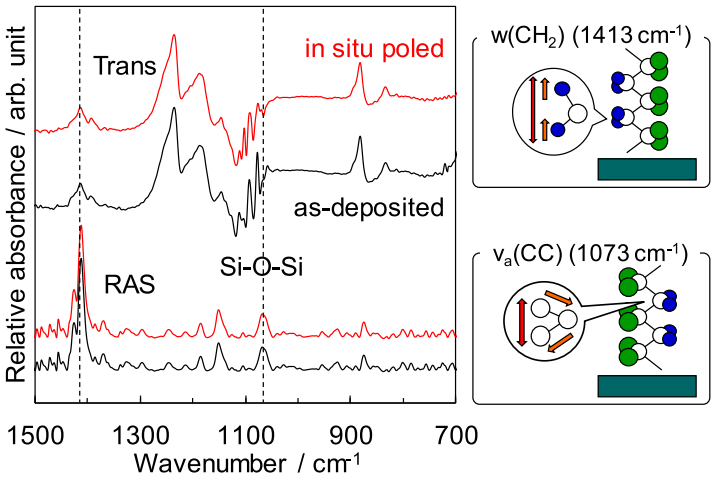

Fig. 4. (Color online) FT-IR transmission and reflection absorption spectra of as-deposited and in situ poled VDF oligomer thin films fabricated by vacuum evaporation.

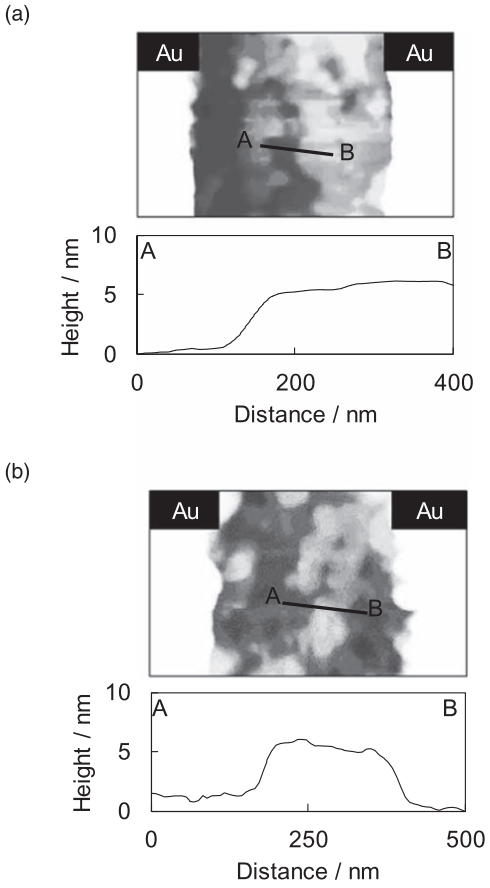

Fig. 5. AFM images of (a) as-deposited and (b) in situ poled VDF oligomer thin films fabricated by vacuum evaporation.

without an electric field [Fig. 5(a)]. Based on the line profile, the height of steps in the AFM image is ~4–5 nm, which corresponds to the length of the single molecule (4.8 nm; the all-trans conformation shows the highest ferroelectricity), and we speculated that the plate-like grains were formed with six layers of perpendicularly oriented VDF oligomer molecules. On the other hand, in the film formed under the influence of an electric field, an anisotropic crystal arrangement in the vicinity of the electrode was occasionally confirmed [Fig. 5(b)], but it was not clear. It has been reported that a VDF oligomer forms hexagonal plate shaped crystals.[14] Distorted hexagonal plate shaped crystals were observed in this study. The deformation of the crystal habit is attributed to the melting of the VDF oligomer due to the high substrate temperature during the vacuum evaporation. However, because the thin films had a P_r of 100 mC m^{-2}, the perpendicularly oriented VDF oligomer could be almost completely poled by the application of a lower electric field (7.7 MV m^{-1}) during the formation of the film than that applied for post-poling (100 MV m^{-1}).

Figure 6(a) shows the time dependence of the output voltage of the in situ poled sensor modulated of infrared radiation by a frequency of 0.2 Hz. As shown in Fig. 6(a), the output voltage increased immediately and rapidly when the sensor was irradiated with infrared radiation, and then decreased gradually. Similarly, the output voltage decreased immediately when the irradiation was stopped. This signal variation corresponding to the infrared ray on/off is a typical behavior of a pyroelectric material. Figure 6(b) shows the voltage sensitivity of the pyroelectric sensor as a function of the frequency of the modulated infrared ray. The voltage sensitivity was calculated in two ways because the irradiated area of the infrared ray was different from the electrode area in the case of the comb-like electrodes. The first one was defined as the electrode area, reading out the pyroelectric signal. The second one was defined as the irradiation of infrared rays, the space area of comb-like electrodes. The value calculated using the electrode area is shown in parentheses. The in situ poled sensor formed with six layers of perpendicularly oriented VDF oligomer molecules showed voltage sensitivity, which reached 198 (3003) V W^{-1} at 1 Hz, and this sensitivity is higher than that of the sensor subjected to post-poling treatment [16 (238) V W^{-1}]. Meanwhile, the conventional sandwich sensor with parallelly oriented VDF oligomers fabricated on a Si substrate (NiCr/VDF/Al/SiO_2/Si) shows a voltage sensitivity of only 72 V W^{-1}, even after post-poling treatment. Originally, the sensitivities of pyroelectric sensors on SiO_2/Si tended to be not good due to the large heat capacity of the substrate. However, note that the sensitivity of the in situ poled sensor was high, although we did not use an absorption layer, typically NiCr or Au-black, which converts irradiated light into heat. Here, the

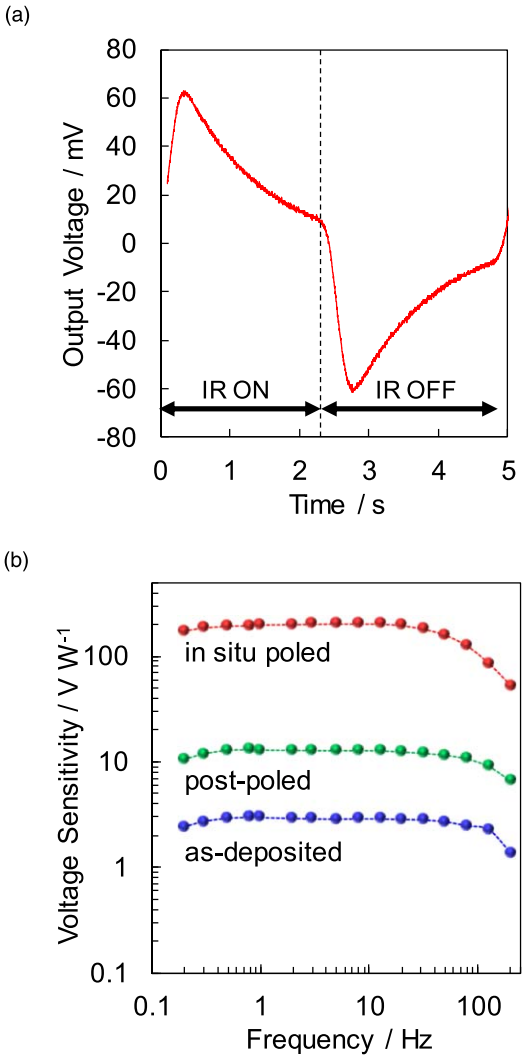

Fig. 6. (Color online) (a) Voltage sensitivity and (b) output voltage of sensors versus the IR frequency.

influence of the method used for polarization and the device configuration on the sensitivity of the sensor was considered. Table I compares the voltage sensitivities of different VDF oligomer pyroelectric sensors fabricated by our group. The voltage sensitivity of the in situ poled sensor decreased after a post-poling treatment. This result suggests that the method used for polarization strongly affects the sensitivity of the sensor. The sensitivity might not only be related to the extent of P_r but also to the poling process. Therefore, we further investigated the charge injection from the electrode to the molecular layer by applying a high electric field for post-poling.

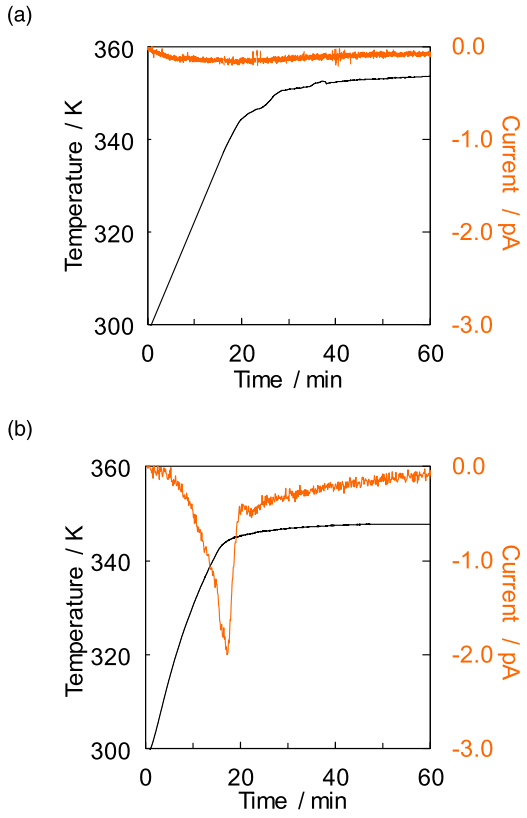

Fig. 7. (Color online) TSC curves of VDF oligomer thin films: (a) in situ poled and (b) post-poled.

Figure 7 shows the TSC curve. The in situ poled sensor shows no peak with increasing temperature [Fig. 7(a)]. On the other hand, the post-poled sensor shows a clear peak with increasing temperature [Fig. 7(b)], indicating charge injection from the comb-like electrode to the VDF oligomer films during the application of high voltage. The origin of the pyroelectricity is the discharge of compensated charges because of the dipole fluctuations with temperature changes in the pyroelectric material. The charge injected into the pyroelectric material, which always occurred at the time of post-poling treatment by the application of a high electric field, disturbed the dipole fluctuation. Therefore, we attribute the difference in voltage sensitivity between the in situ poled and post-poled sensors to the injection of charges. In post-poling treatment, the injected charges disturbed the dipole fluctuation and pyroelectric response [Fig. 8(b)]. By contrast, when a low electric field was applied during vacuum evaporation, charge injection was suppressed. Meanwhile, the magnitude of the electric field was adequate to drive the

Table I. Comparison of the voltage sensitivities of VDF oligomer based sensors.

Orientation		Perpendicular				Parallel	
Thickness		30 nm (six layers)				1.3 μm	
Substrate		SiO_2/Si				SiO_2/Si	Plastic films
Device configuration		Comb-like structure (Au)				Sandwich structure (NiCr/VDF/Al)	
In situ poled		○		×		×	×
Post-poled		×	○	×	○	○	○
Voltage sensitivity (@ 1 Hz)	Calculated by irradiation area	198	15	3	16	72	1000
	Calculated by electrode area	3003	228	46	238		

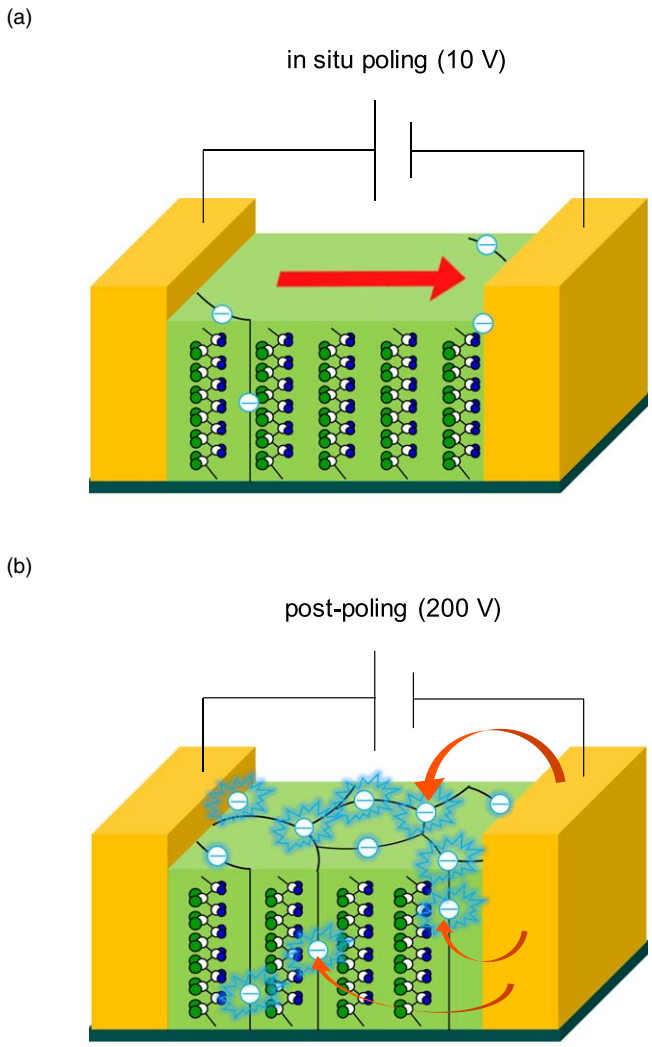

Fig. 8. (Color online) Overview of the charge injection of VDF oligomer thin films: (a) in situ poled and (b) post-poled.

alignment of the dipoles of the VDF oligomer in the gaseous state. The sensor therefore exhibited an extremely high voltage sensitivity [Fig. 8(a)]. The results indicate that even if a thin film is prepared with less injected charge in in situ poling, the sensitivity of the sensor decreases due to the influence of the injected charge, although the amount of remanent polarization is increased by post-poling. Thus, we found that reducing the voltage during the poling treatment and thereby reducing the charge injected into the film is important for improving the sensitivity of the pyroelectric sensor.

Despite using a film with a few molecular layers, in this study, the pyroelectric response could be observed without the use of an infrared ray absorption layer. In recent years, much research has been conducted on plasmonic structures that considerably increase the infrared absorption efficiency based on the plasmon resonance that appears on the surface of microstructured metals.[28–32] Because the structure of a comb-like electrode is similar to that of the wire grid used in a polarizer, the micro-gapped comb-like electrode used in this study is expected to facilitate improved infrared absorption rates. Including the possibility of infrared absorption described above, the results confirm that in situ poling enables the formation of highly pure thin films with low injected charge and is useful for the fabrication of pyroelectric sensors.

4. Conclusions

The dipoles of the VDF oligomers were highly oriented between the micro-gapped comb-like electrodes in the in-plane direction with perpendicular molecular ordering and high crystallinity. A high electric field was not necessary for achieving the orientation of the molecular dipole, because of the effective alignment of the dipoles of the VDF oligomer in the highly mobile gaseous state under the applied electric field. The pyroelectric sensor based on a VDF oligomer thin film deposited under the influence of a low electric field showed increased output voltage due to the suppression of charge injection. Moreover, because the sensor showed a pyroelectric response, although a film with a few molecular layers was used, we predict improvements in the infrared absorption rate and infrared ray–heat conversion by adopting a fine electrode structure. Our findings will enable the easy and effective fabrication of high-performance pyroelectric sensors, allowing the exploitation of organic ferroelectrics as new components of nontoxic pyroelectric sensing devices in the future.

Acknowledgments

This research was partly supported by a Grant-in-Aid for Scientific Research from JSPS KAKENHI, CREST form JST, and the Kyoto University Nano Technology Hub under the “Nanotechnology Platform Project” sponsored by MEXT, Japan.

1) J. Gao, L. Lei, and S. Yu, Big data sensing and service: a tutorial. IEEE 1st Int. Conf. Big Data Computing Service and Applications 2015, 79.
2) S. Cha, A. Abusharekh, and S. S. R. Abidi, Towards a “big” health data analytics platform. IEEE 1st Int. Conf. Big Data Computing Service and Applications 2015, 233.
3) J. Yang, From Google File System to Omega: a decade of advancement in big data management at Google. IEEE 1st Int. Conf. Big Data Computing Service and Applications 2015, 249.
4) L. Deng, J. Gao, and C. Vuppalapati, Building a big data analytics service framework for mobile advertising and marketing. IEEE 1st Int. Conf. Big Data Computing Service and Applications 2015, 256.
5) Q. Hao, D. J. Brady, B. D. Guenther, J. B. Burchett, M. Shankar, and S. Feller, IEEE Sens. J. **6**, 1683 (2006).
6) P. Zappi, E. Farella, and L. Benini, IEEE Sens. J. **10**, 1486 (2010).
7) C. Christofides and A. Mandelis, J. Appl. Phys. **68**, R1 (1990).
8) F. Erden, B. U. Toreyin, E. B. Soyer, I. Inac, O. Gunay, K. Kose, and A. E. Cetin, Fire Saf. J. **53**, 13 (2012).
9) R. Köhler, N. Neumann, N. Heß, R. Bruchhaus, W. Wersing, and M. Simon, Ferroelectrics **201**, 83 (1997).
10) M. Schreiter, R. Bruchhaus, D. Pitzer, and W. Wersing, Sputtering of self-polarized PZT films for IR-detector arrays. Proc. 11th IEEE Int. Symp. Applications of Ferroelectrics 1998, 181.
11) Y. Kuroda, Y. Koshiba, M. Misaki, K. Ishida, and Y. Ueda, Appl. Phys. Express **6**, 021601 (2013).
12) I. R. Mahdi, C. W. Gan, and H. A. W. Majid, Sensors **14**, 19115 (2014).
13) K. Noda, K. Ishida, A. Kubono, T. Horiuchi, H. Yamada, and K. Matsushige, J. Appl. Phys. **93**, 2866 (2003).
14) T. Inoue, A. Mori, Y. Koshiba, M. Misaki, and K. Ishida, Appl. Phys. Express **8**, 111601 (2015).
15) K. Noda, K. Ishida, T. Horiuchi, H. Yamada, and K. Matsushige, Jpn. J. Appl. Phys. **42**, L1334 (2003).
16) M. D. Aggarwal, A. K. Batra, P. Guggilla, M. E. Edwards, B. G. Penn, and J. R. Currie, Aeronaunt. Sp. Adm. Tech. Rep. NASA/TM-2010-216373 NASA, 2010.
17) S. K. Dey, K. D. Budd, and D. A. Payne, IEEE Trans. Ultrason. Ferroelectr. Freq. Control **35**, 80 (1988).
18) Y. Ueda and M. Ashida, J. Electron Microsc. **29**, 38 (1980).

19) K. Fukao, T. Horiuchi, and K. Matsushige, Thin Solid Films **171**, 359 (1989).
20) K. Noda, K. Ishida, T. Horiuchi, K. Matsushige, and A. Kubono, J. Appl. Phys. **86**, 3688 (1999).
21) S. Kuwajima, S. Horie, T. Horiuchi, H. Yamada, K. Matsushige, and K. Ishida, Macromolecules **42**, 3353 (2009).
22) Y. Yoshida, T. Horiuchi, and K. Matsushige, Jpn. Appl. Phys. **32**, 1248 (1993).
23) A. Takeno, N. Okui, T. Kitoh, M. Muraoka, S. Umemoto, and T. Sakai, Thin Solid Films **202**, 213 (1991).
24) D. H. Chang and Y. S. Yoon, Jpn. J. Appl. Phys. **41**, 7234 (2002).
25) M. Kobayashi, K. Tashiro, and H. Tadokoro, Macromolecules **8**, 158 (1975).
26) K. Tashiro, Y. Abe, and M. Kobayashi, Ferroelectrics **171**, 281 (1995).
27) A. M. Bachmann, L. W. Gordon, L. J. Koenig, and B. J. Lando, J. Appl. Phys. **50**, 6106 (1979).
28) W. T. Ebbesen, J. H. Lezec, F. H. Ghaemi, T. Thio, and A. P. Wolff, Nature **391**, 667 (1998).
29) L. J. Gall, M. Olivier, and J. J. Greffet, Phys. Rev. B **55**, 10105 (1997).
30) K. Ikeda, H. T. Miyazaki, T. Kasaya, K. Yamamoto, Y. Inoue, K. Fujimura, T. Kanakugi, M. Okada, K. Hatade, and S. Kitagawa, Appl. Phys. Lett. **92**, 021117 (2008).
31) F. Kusa, I. Morichika, A. Takegami, and S. Ashihara, Opt. Express **25**, 12896 (2017).
32) S. Ogawa and M. Kimata, Opt. Mater. Express **7**, 633 (2017).